Learning the Minimum Action Distance

Anonymous Author(s)
Affiliation
Address
email

Abstract

This paper presents a state representation framework for Markov decision processes (MDPs) that can be learned solely from state trajectories, requiring neither reward signals nor the actions executed by the agent. We propose learning the *minimum action distance* (MAD), defined as the minimum number of actions required to transition between states, as a fundamental metric that captures the underlying structure of an environment. MAD naturally enables critical downstream tasks such as goal-conditioned reinforcement learning and reward shaping by providing a dense, geometrically meaningful measure of progress. Our self-supervised learning approach constructs an embedding space where the distances between embedded state pairs correspond to their MAD, accommodating both symmetric and asymmetric approximations. We evaluate the framework on a comprehensive suite of environments with known MAD values, encompassing both deterministic and stochastic dynamics, as well as discrete and continuous state spaces, and environments with noisy observations. Empirical results demonstrate that the proposed approach not only efficiently learns accurate MAD representations across these diverse settings but also significantly outperforms existing state representation methods in terms of representation quality.

1 Introduction

In reinforcement learning (Sutton and Barto, 1998), an agent aims to learn useful behaviors through continuing interaction with its environment. Specifically, by observing the outcomes of its actions, a reinforcement learning agent learns over time how to select actions in order to maximize the expected cumulative reward it receives from its environment. An important need in applications of reinforcement learning is the ability to generalize, not only to previously unseen states, but also to variations of its environment that the agent has not previously interacted with.

In many applications of reinforcement learning, it is useful to define a metric that measures the similarity of two states in the environment. Such a metric can be used, e.g., to define equivalence classes of states in order to accelerate learning, to decompose the problem into a hierarchy of smaller subproblems that are easier to solve, or to perform transfer learning in case the environment changes according to some parameters but retains part of the structure of the original environment. Such a metric can also be used as a heuristic in goal-conditioned reinforcement learning, in which the agent has to achieve different goals in the same environment.

The Minimum Action Distance (MAD) has proved useful as a similarity metric, with applications in various areas of reinforcement learning, including policy learning (Wang et al., 2023; Park et al., 2023), reward shaping (Steccanella and Jonsson, 2022), and option discovery (Park et al., 2024a,b). While prior work has demonstrated the advantages of using MAD, how best to approximate it remains an open problem. Existing methods have not been systematically evaluated on their ability to approximate the MAD function itself, and many rely on symmetric approximations, even though the true MAD is inherently asymmetric.

Submitted to the 18th European Workshop on Reinforcement Learning (EWRL 2025). Do not distribute.

We make three main contributions towards fast, accurate approximation of the MAD. First, we propose two novel algorithms for learning MAD using only state trajectories collected by an agent interacting with its environment. Unlike previous work, the proposed algorithms naturally support both symmetric and asymmetric distances, and incorporate both short- and long-term information about how distant two states are from one another. Secondly, we define a novel quasimetric distance function that is computationally efficient and that, in spite of its simplicity, outperforms more elaborate quasimetrics in the existing literature. Finally, we introduce a diverse suite of environments — including those with discrete and continuous state spaces, stochastic and deterministic dynamics, and directed and undirected transitions — in which the ground-truth MAD is known, enabling a systematic and controlled evaluation of different MAD approximation methods.

Figure 1 illustrates the steps of MAD representation learning: an agent collects state trajectories from an unknown environment, which are used to learn a state embedding that implicitly defines a distance function between states.

2 Related Work

In applications such as goal-conditioned reinforcement learning (Ghosh et al., 2020) and stochastic shortest-path problems (Tarbouriech et al., 2021), the temporal distance is measured as the expected number of steps required to reach one state from another state under some policy. In contrast, the MAD is a lower bound on the number of steps, rather than an expectation. The main benefits are that the MAD is efficient to compute and invariant to changes in the transition probabilities as long as the support over next states remains the same, making it suitable for representation learning and transfer learning.

Prior work has explored the connection between the MAD and optimal goal-conditioned value functions (Kaelbling, 1993). Park et al. (2023) highlight this connection and propose a hierarchical approach that improves distance estimates over long horizons. Park et al. (2024a) embed states into a learned latent space where the distance between embedded states directly reflects an on-policy measure of the temporal distance (Hartikainen et al., 2020). Park et al. (2024b) extend this to the offline setting, learning a Hilbert space embedding from arbitrary experience data such that Euclidean distances between state embeddings approximate the MAD. Steccanella and Jonsson (2022) Propose a method for learning a distance function that approximates the MAD, but relies on a symmetric distance metric, which limits its ability to capture directional structure in the environment.

A common limitation of these existing approaches is that they lead to symmetric distance metrics, which cannot capture the asymmetry of the true MAD in environments with irreversible dynamics. In contrast, our proposed approach supports the use of asymmetric distance metrics (or, *quasimetrics*), which can better capture the directional structure in many environments.

Prior work has also explored the use of quasimetrics in reinforcement learning. Wang et al. (2023) proposes a method for learning a distance function that approximates the MAD. Their formulation, similarly to our work, is based on the idea of preserving local structure while learning a global distance function. Unlike our proposed approach, however, their method does not leverage the existing distance along a trajectory as supervision for the learning process, and they rely on the use of Interval Quasimetric Embedding (IQE) (Wang and Isola, 2022) to learn the distance function.

Similar to our work, Dadashi et al. (2021) learn embeddings and define a pseudometric between two states as the Euclidean distance between their embeddings. Unlike our work, an embedding is computed both for the state-action space and the state space, and the embeddings are trained using loss functions inspired by bisimulation.

Prior work has also proposed the use of successor features (Dayan, 1993; Barreto et al., 2017) and time-contrastive representations (Eysenbach et al., 2022) as the basis for learning distance metrics. Myers et al. (2024) introduce time-contrastive successor features, defining a distance metric based on the difference between discounted future occupancies of state features learned via time-contrastive learning. While their metric satisfies the triangle inequality and naturally handles both stochasticity and asymmetry, the resulting distances reflect expected discounted state visitations under a specific behavior policy and lack an intuitive interpretation. In contrast, approaches that approximate the MAD are naturally interpretable as a lower bound on the number of actions needed to transition between two states.

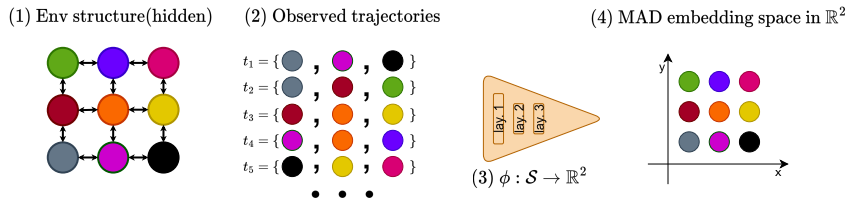

Figure 1: Schematic overview of MAD representation learning. From left to right: (1) the hidden environment graph, (2) trajectories collected by an unknown policy, (3) the embedding function $\phi : S \to \mathbb{R}^2$ and (4) the resulting MAD embedding space in $\mathbb{R}^2$.

3 Background

In this section, we introduce notation and concepts that are used throughout the paper. Given a finite set $\mathcal{X}$, we use $\Delta(\mathcal{X}) = \{p \in \mathbb{R}^{\mathcal{X}} \mid \sum_x p_x = 1, p_x \geq 0\,(\forall x)\}$ to denote the probability simplex, i.e. the set of all probability distributions over $\mathcal{X}$. A rectified linear unit (ReLU) is a function $\mathrm{relu} : \mathbb{R}^d \to \mathbb{R}^d$ defined on any vector $x \in \mathbb{R}^d$ as $\mathrm{relu}(x) = \max(0, x)$.

Markov Decision Processes (MDPs). An MDP is a tuple $\mathcal{M} = \langle \mathcal{S}, \mathcal{A}, \mathcal{R}, \mathcal{P} \rangle$, where $\mathcal{S}$ is the state space, $\mathcal{A}$ is the action space, $\mathcal{R} : \mathcal{S} \times \mathcal{A} \to \mathbb{R}$ is the reward function, and $\mathcal{P} : \mathcal{S} \times \mathcal{A} \to \Delta(\mathcal{S})$ is the transition kernel. At each time t, the learning agent observes a state $s_t \in \mathcal{S}$, selects an action $a_t \in \mathcal{A}$, receives a reward $r_t = \mathcal{R}(s_t, a_t)$ and transitions to a new state $s_{t+1} \sim \mathcal{P}(s_t, a_t)$. The learning agent selects actions using a policy $\pi : \mathcal{S} \to \Delta(\mathcal{A})$, i.e. a mapping from states to probability distributions over actions. In our work, the state space $\mathcal{S}$ can be either discrete or continuous.

Reinforcement learning (RL). RL is a family of algorithms whose purpose is to learn a policy π that maximizes some measure of expected future reward. In the present paper, however, we consider the problem of representation learning, and hence we are not directly concerned with the problem of learning a policy. Concretely, we wish to learn a distance function between pairs of states that can later be used by an RL agent to learn more efficiently. In this setting, we assume that the learning agent uses a behavior policy π_b to collect trajectories. Since we are interested in learning a distance function over state pairs, actions are relevant only for determining possible transitions between states, and rewards are not relevant at all. Hence for our purposes a trajectory $\tau = (s_0, s_1, \ldots, s_n)$ is simply a sequence of states.

4 The Minimum Action Distance.

Given an MDP $\mathcal{M} = \langle \mathcal{S}, \mathcal{A}, \mathcal{R}, \mathcal{P} \rangle$ and a state pair $(s, s') \in \mathcal{S}^2$, the Minimum Action Distance $d_\mathrm{MAD}(s, s')$, is defined as the minimum number of decision steps needed to transition from s to s'. In deterministic MDPs, the MAD is always realizable using an appropriate policy; in stochastic MDPs, the MAD is a lower bound on the actual number of decision steps of any policy. Let $R \subseteq \mathcal{S}^2$ be a relation such that $(s, s') \in R$ if and only if there exists an action $a \in \mathcal{A}$ that satisfies $\mathcal{P}(s'|s, a) > 0$. Hence R contains all state pairs (s, s') such that s' is reachable in one step from s. We can formulate the problem of computing d_MAD as a constrained optimization problem:

$$
\begin{aligned}
d_\mathrm{MAD} = \arg\max_{d} & \sum_{(s,s') \in \mathcal{S}^2} d(s, s'), && (1)\\
\text{s.t.} \quad & d(s, s) = 0 \quad \forall s \in \mathcal{S}, \\
& d(s, s') \leq 1 \quad \forall (s, s') \in R, \\
& d(s, s') \leq d(s, s'') + d(s'', s') \quad \forall (s, s', s'') \in \mathcal{S}^3.
\end{aligned}
$$

It is straightforward to show that d_MAD is the unique solution to equation 1. Concretely, d_MAD satisfies the second constraint with equality, i.e. $d(s, s') = 1$ for all $(s, s') \in R$. If the state space $\mathcal{S}$ is finite, the constrained optimization problem is precisely the linear programming formulation of the all-pairs shortest path problem for the graph $(\mathcal{S}, R)$ with edge costs 1. This graph is itself a determinization of the MDP $\mathcal{M}$ (Yoon et al., 2007). In this case we can compute d_MAD exactly using the well-known Floyd-Warshall algorithm (Floyd, 1962; Warshall, 1962). If the state space $\mathcal{S}$ is continuous, R is still

well-defined, and hence there still exists a solution which satisfies $d(s, s') = 1$ for all $(s, s') \in R$ even though the states can no longer be enumerated.

An alternative to the MAD is to compute the stochastic shortest path (SSP) (Tarbouriech et al., 2021) between each pair of states. However, the linear programming formulation of the all-pairs SSP problem involves transition probabilities, which makes the constrained optimization problem significantly harder to solve. In deterministic MDPs, MAD and SSP are equivalent. In stochastic MDPs, SSP provides a better distance estimate than MAD when some transitions have very small probabilities; however, in many domains, MAD is still a good approximation, e.g. in navigation problems and when using sticky actions. Moreover, the MAD is invariant to changes in the transition probabilities as long as the support of the transition probabilities remain the same, making it especially useful for transfer learning. As already mentioned, the MAD has proven useful in various applications in previous work (Wang et al., 2023; Park et al., 2023; Steccanella and Jonsson, 2022; Park et al., 2024a,b).

Even when the state space $\mathcal{S}$ is finite, we may not have explicit knowledge of the relation R. In addition, the time complexity of the Floyd-Warshall algorithm is $O(|\mathcal{S}|^3)$, and the number of states may be too large to run the algorithm in practice. If the state space $\mathcal{S}$ is continuous, then we cannot even explicitly form a graph $(\mathcal{S}, R)$. Hence we are interested in estimating d_{MAD} in the setting for which we can access trajectories only through sampling. For this purpose, let us assume that the learning agent uses a behavior policy π_{b} to collect a dataset of trajectories $\mathcal{D} = \{\tau_1, \ldots, \tau_k\}$. Define $\mathcal{S}_{\mathcal{D}} \subseteq \mathcal{S}$ as the subset of states that appear on any trajectory in $\mathcal{D}$. Given a trajectory $\tau = \{s_0, ..., s_n\}$ and any two states s_i and s_j on the trajectory such that $0 \leq i < j \leq n$, it is easy to see that $j - i$ is an upper bound on $d_{\text{MAD}}(s_i, s_j)$, since s_j is reachable in $j - i$ steps from s_i on the trajectory τ. By an abuse of notation, we often write $(s_i, s_j) \in \tau$ to refer to a state pair on the trajectory τ with indices i and j such that $i < j$, and we write $(s_i, s_j) \sim \tau$ in order to sample two such states from τ.

Steccanella and Jonsson (2022) learn a parameterized state embedding $\phi_\theta : \mathcal{S} \to \mathbb{R}^d$ and define a distance function $d_\theta(s, s') = d(\phi_\theta(s), \phi_\theta(s'))$, where d is any distance metric in Cartesian space. The parameter vector θ of the state embedding is learned by minimizing the loss function

$$\mathcal{L} = \mathbb{E}_{\tau \sim \mathcal{D}, (s_i, s_j) \sim \tau} \left[(d_\theta(s_i, s_j) - (j - i))^2 + w_c \cdot \text{relu}(d_\theta(s_i, s_j) - (j - i))^2 \right], \tag{2}$$

where $w_c > 0$ is a regularization factor that multiplies a penalty term which substitutes the upper bound constraints $d_\theta(s_i, s_j) \leq j - i$. If the distance metric d satisfies the triangle inequality (e.g. any norm $d = ||\cdot||_p$) then the constraints $d_\theta(s, s) = 0$ and the triangle inequality automatically hold. Enforcing the constraint $d_\theta(s_i, s_j) \leq j - i$ for each state pair (s_i, s_j) on trajectories, rather than only consecutive pairs, helps learn better distance estimates, at the cost of a larger number of constraints.

5 Asymmetric Distance Metrics.

A limitation of previous work is that the chosen distance metric d is symmetric, while the MAD d_{MAD} may not be symmetric. In this section, we review several asymmetric distance metrics. Concretely, a quasimetric is a function $d_q : \mathbb{R}^d \times \mathbb{R}^d \to \mathbb{R}_+$ that satisfies the following three conditions:

- **Q1** (Identity): $d_q(x, x) = 0$.
- **Q2** (Non-negativity): $d_q(x, y) \geq 0$.
- **Q3** (Triangle inequality): $d_q(x, z) \leq d_q(x, y) + d_q(y, z)$.

A quasimetric does not require symmetry, i.e. $d_q(x, y) = d_q(y, x)$ does not hold in general.

We define a simple quasimetric d_{simple} using rectified linear units:

$$d_{\text{simple}}(x, y) = \alpha \max(\text{relu}(x - y)) + (1 - \alpha) \frac{1}{d} \sum_i^d \text{relu}(x_i - y_i). \tag{3}$$

This metric is a weighted average of the maximum and average positive difference between the vectors x and y along any dimension, where $\alpha \in [0, 1]$ is a weight. In Appendix A, we show that d_{simple} satisfies the triangle inequality and latent positive homogeneity (Wang and Isola, 2022).

The Wide Norm quasimetric (Pitis et al., 2020), d_{WN}, applies a learned transformation to an asymmetric representation of the difference between two states. The Wide Norm is defined as

$$d_{\text{WN}}(x, y) = ||W(\text{relu}(x - y) :: \text{relu}(y - x))||_2,$$

where "::" denotes concatenation and $W \in \mathbb{R}^{k \times 2d}$ is a learned weight matrix. This ensures that $d_{\text{WN}}(x, y)$ is non-negative and satisfies the triangle inequality, while concatenation is asymmetric.

The Interval Quasimetric Embedding (IQE) (Wang and Isola, 2022) leverages the Lebesgue measure of interval unions to capture asymmetric distances. Rather than vectors, IQE is defined on matrices $X, Y \in \mathbb{R}^{k \times m}$. Let x_{ij} denote the element in row i and column j of matrix X. For each row i, we construct an interval by taking the union over the intervals defined by matrices X and Y:

$$I_i(X, Y) = \bigcup_{j=1}^{m} \left[x_{ij},\, \max\{x_{ij},\, y_{ij}\} \right].$$

The length of this interval, denoted by $L_i(X, Y)$, is computed as its Lebesgue measure. The IQE distance is obtained by aggregating these row-wise lengths. For example, one may define

$$d_{\text{IQE}}(X, Y) = \sum_{i=1}^{k} L_i(X, Y),$$

or, alternatively, using a maxmean reduction:

$$d_{\text{IQE-mm}}(X, Y) = \alpha \max_{1 \le i \le k} L_i(X, Y) + (1 - \alpha) \frac{1}{k} \sum_{i=1}^{k} L_i(X, Y),$$

where $\alpha \in [0, 1]$ balances the influence of the maximum and the average. This construction yields a quasimetric that inherently respects the triangle inequality while accounting for directional differences between the matrices X and Y.

Given any of the above quasimetrics d_q (i.e. d_{simple}, d_{WN} or d_{IQE}), we can now define an asymmetric distance function $d_\theta(s, s') = d_q(\phi_\theta(s), \phi_\theta(s'))$. In the case of d_{IQE}, the state embedding $\phi : \mathcal{S} \to \mathbb{R}^{k \times m}$ has to produce a matrix rather than a vector. The choice of quasimetric directly shapes the trade-offs in computational cost and optimization dynamics. In Appendix C, we present an ablation study examining how this choice affects our algorithms.

6 Learning Asymmetric MAD Estimates

In this section we propose two novel variants of the MAD learning approach, each training an state encoding ϕ_θ that maps states to an embedding space, and using a quasimetric d_q to compute distances $d_\theta(s, s') = d_q(\phi_\theta(s), \phi_\theta(s'))$ between state pairs (s, s'). Both variants support any quasimetric formulation such as d_{simple}, d_{WN} and d_{IQE}, and can incorporate additional features such as gradient clipping.

6.1 MadDist: Direct Distance Learning

The first algorithm, which we call MadDist, learns state distances using an approach similar to prior work Steccanella and Jonsson (2022), but differs in the use of a quasimetric distance function and a scale-invariant loss. Concretely, MadDist minimizes the following composite loss function:

$$\mathcal{L} = \mathcal{L}_o + w_r \mathcal{L}_r + w_c \mathcal{L}_c. \tag{4}$$

The main objective, $\mathcal{L}_o$, is a scaled version of the square difference in equation 2:

$$\mathcal{L}_o = \mathbb{E}_{\tau \sim \mathcal{D}, (s_i, s_j) \sim \tau} \left[\left(\frac{d_\theta(s_i, s_j)}{j - i} - 1 \right)^2 \right]. \tag{5}$$

Crucially, scaling makes the loss invariant to the magnitude of the estimation error, which typically increases as a function of $j - i$. In other words, states that are further apart on a trajectory do not necessarily dominate the loss simply because the magnitude of the estimation error is larger.

The second loss term, $\mathcal{L}_r$, which is weighted by a factor $w_r > 0$, is a contrastive loss that encourages separation between state pairs randomly sampled from all trajectories:

$$\mathcal{L}_r = \mathbb{E}_{(s, s') \sim \mathcal{S}_\mathcal{D}} \left[\text{relu} \left(1 - \frac{d_\theta(s, s')}{d_{\text{max}}} \right)^2 \right] \tag{6}$$

where $d_{\max}$ is a hyperparameter. Finally, the loss term $\mathcal{L}_c$, which is weighted by a factor $w_c > 0$, enforces the upper bound constraints. Specifically, let $\mathcal{D}_{\leq H_c}$ denote the set of state pairs sampled from trajectories in $\mathcal{D}$ such that the index difference satisfies $1 \leq j - i \leq H_c$, i.e.

$$\mathcal{D}_{\leq H_c} = \{(s_i, s_j) \,|\, \tau \in \mathcal{D},\ s_i, s_j \in \tau,\ 1 \leq j - i \leq H_c\}\,.$$

Then, the constraint loss is defined as:

$$\mathcal{L}_c = \mathbb{E}_{(s_i,s_j)\sim\mathcal{D}_{\leq H_c}}\left[\text{relu}\left(d_\theta(s_i, s_j) - (j - i)\right)^2\right]. \tag{7}$$

where H_c is a hyperparameter.

6.2 TDMadDist: Temporal Difference Learning

The second algorithm, which we call *TDMadDist*, incorporates temporal difference learning principles by maintaining a separate target embedding $\phi_{\theta'}$ and learning via bootstrapped targets. Specifically, TDMadDist learns by minimizing the loss function $\mathcal{L}' = \mathcal{L}'_o + w_r\mathcal{L}'_r + w_c\mathcal{L}_c$, where $\mathcal{L}_c$ is the loss term from equation 7 that enforces the upper bound constraints.

The main objective $\mathcal{L}'_o$ of TDMadDist is modified to include bootstrapped distances:

$$\mathcal{L}'_o = \mathbb{E}_{\tau\sim\mathcal{D},(s_i,s_j)\sim\tau}\left[\left(\frac{d_\theta(s_i, s_j)}{\min(j - i, 1 + d_{\theta'}(s_{i+1}, s_j))} - 1\right)^2\right]. \tag{8}$$

Hence if the current distance estimate $d_{\theta'}(s_{i+1}, s_j)$ computed using the target embedding $\phi_{\theta'}$ is smaller than $j - (i + 1)$, the objective is to make $d_\theta(s_i, s_j)$ equal to $1 + d_{\theta'}(s_{i+1}, s_j)$.

We also modify the second loss term $\mathcal{L}'_r$ to include bootstrapped distances:

$$\mathcal{L}'_r = \mathbb{E}_{\tau\sim\mathcal{D},(s_i,s_j)\sim\tau,s_r\sim\mathcal{S}_\mathcal{D}}\left[\left(\frac{d_\theta(s_i, s_r)}{1 + d_{\theta'}(s_{i+1}, s_r)} - 1\right)^2\right]. \tag{9}$$

Given a state s_i sampled from a trajectory of $\mathcal{D}$ and a random state $s_r \in \mathcal{S}_\mathcal{D}$, the objective is to make $d_\theta(s_i, s_r)$ equal to $1 + d_{\theta'}(s_{i+1}, s_r)$.

The target network parameters θ' are updated in each time step via an exponential moving average:

$$\theta' \leftarrow (1 - \beta)\theta' + \beta\theta, \tag{10}$$

where $\beta \in (0, 1)$ is a hyperparameter.

7 Experiments

We evaluate our proposed MAD learning algorithms on a diverse set of environments with varying characteristics, including deterministic and stochastic dynamics, discrete and continuous state spaces, and environments with noisy observations. Our experiments are designed to address the following questions:

- How accurately do our learned embeddings capture the true minimum action distances?
- How does the performance of our method compare to existing quasimetric learning approaches?
- How robust is our approach to environmental stochasticity and observation noise?

Evaluation Metrics. We evaluate the quality of our learned representations using three metrics:

- **Spearman Correlation** (ρ): Measures the preservation of ranking relationships between state pairs. A high Spearman correlation indicates that if state s_i is farther from state s_j than from state s_k in the true environment, our learned metric also predicts this same ordering. Perfect preservation of distance rankings gives $\rho = 1$.
- **Pearson Correlation** (r): Measures the linear relationship between predicted and true distances. A high Pearson correlation indicates that our learned distances scale proportionally with true distances - when true distances increase, our predictions increase linearly as well. Perfect linear correlation gives $r = 1$.

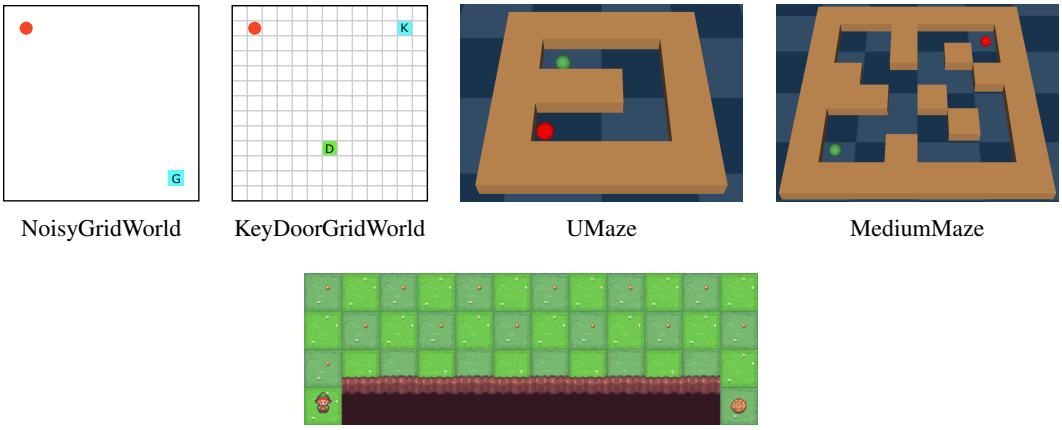

NoisyGridWorld KeyDoorGridWorld UMaze MediumMaze

CliffWalking

Figure 2: The environments used in our analysis.

- **Ratio Coefficient of Variation (CV)**: Measures the consistency of our distance scaling across different state pairs. A low CV indicates that our predicted distances maintain a consistent ratio to true distances throughout the state space. For example, if we consistently predict distances that are approximately 1.5 times the true distance, CV will be low. High variation in this ratio across different state pairs results in high CV. More formally, given a set of ground truth distances $d_1, d_2, ..., d_n$ and their corresponding predicted distances $\hat{d}_1, \hat{d}_2, ..., \hat{d}_n$ where $d_i > 0$, we compute the ratios $r_i = \hat{d}_i / d_i$. The Ratio CV is given by

$$CV = \frac{\sigma_r}{\mu_r} = \frac{\sqrt{\frac{1}{n}\sum_{i=1}^{n}(r_i - \mu_r)^2}}{\frac{1}{n}\sum_{i=1}^{n} r_i}, \tag{11}$$

Baselines. We compare our methods against QRL (Wang et al., 2023), a recent quasimetric reinforcement learning approach that learns state representations using the Interval Quasimetric Embedding (IQE) formulation. QRL employs a Lagrangian optimization scheme where the objective maximizes the distance between states while maintaining locality constraints.

We also compare against the approach by Park et al. (2024b), an offline reinforcement learning method that embeds states into a learned Hilbert space. In this space, the distance between embedded states approximates the MAD, leading to a symmetric distance metric that cannot capture the natural asymmetry of the true MAD. We include this comparison to demonstrate the benefits of methods that explicitly model the quasimetric nature of the MAD over those that do not.

Environments. To evaluate the proposed methods, we designed a suite of environments where the true MAD is known, enabling a precise quantitative assessment of our learned representations. This perfect knowledge of the ground truth distances allows us to rigorously evaluate how well different algorithms recover the underlying structure of the environment. The environments are illustrated in Figure 2, with full details provided in Appendix D.

Our test environments span a comprehensive range of MDP characteristics:

- **NoisyGridWorld**: A continuous grid world environment with stochastic transitions. The agent can move in four cardinal directions, but the action may fail with a small probability, causing the agent to remain in the same state. The initial state is random and the goal is to reach a target state. The MAD is known and can be computed as the Manhattan distance between states. Moreover we included random noise in the observations by extending the state (x, y) with a random vector of size two resulting in a 4-dimensional state space, where the first two dimensions are the original coordinates and the last two dimensions correspond to noise.
- **KeyDoorGridWorld**: A discrete grid world environment where the agent must find a key to unlock a door. The agent can move in four cardinal directions and the state (x, y, k) is represented by the agent's position (x, y) and whether or not it has the key (k). The MAD is known and can be computed as the Manhattan distance between states where the distance between a state without

the key and a state with the key is the sum of the distances to the key. The key can only be picked up and never dropped creating a strong asymmetry in the distance function.

- **CliffWalking**: The original CliffWalking environment as described by Sutton and Barto (1998). The agent starts at the leftmost state and must reach the rightmost state while avoiding falling off the cliff. If the agent falls it returns to the starting state but the episode is not reset. This creates a strong asymmetry in the distance function, as the agent can take the shortcut by falling off the cliff to move between states.
- **PointMaze**: A continuous maze environment where the agent must navigate through a series of walls to reach a goal (Fu et al., 2020). The task in the environment is for a 2-DoF ball that is force-actuated in the Cartesian directions x and y, to reach a target goal in a closed maze. The underlying maze is a 2D grid with walls and obstacles, that we use in our experiments to approximate the ground truth MAD, by computing the all pairs shortest path using the Floyd-Warshall algorithm over the maze graph. We consider two variants of this environment: **UMaze** and **MediumMaze**.

Empirical Setup. We compared our two algorithms MADDist (MAD) and TDMADDist (TDMAD) against the QRL and Hilbert baselines. Each method was trained for $50{,}000$ gradient steps on an offline dataset gathered by a random policy. For the CliffWalking, NoisyGridWorld, and KeyDoor environments, we used 100 trajectories; for the PointMaze environments, we increased this to 1000 trajectories. All reported results are averages over five independent runs (random seeds) to ensure statistical robustness. For full implementation details of our evaluation setup, see Appendix B.
Figure 3 reports, for each algorithm and environment, the Pearson correlation and coefficient of variation (CV) ratio. We found that Spearman correlations closely match the Pearson results; these are included for completeness in Appendix C, alongside additional ablation studies. The complete codebase for reproducing our experiments will be made public upon acceptance of this paper.

Discussion. From the results in Figure 3, we can see that our proposed methods outperform the QRL and Hilbert baselines in all environments, being able to learn a more accurate approximation of the MAD. This is especially evident in the PointMaze and MediumMaze environments, characterized by a large number of states and a complex structure that makes it hard for a simple random policy to explore the environment accurately. In these environments, QRL fails to learn a good approximation of the MAD, producing smaller values for the Spearman and Pearson correlation metrics and higher values for the Ratio CV metric. This is likely due to the fact that QRL only uses the locality constraints to learn the embeddings, while our methods take advantage of the information contained in the trajectory distances to learn a more accurate approximation of the MAD. The Hilbert baseline performs poorly in highly asymmetric environments like CliffWalking and KeyDoorGridWorld because its symmetric distance formulation cannot capture the directional properties of the MAD.

8 Conclusion

In this paper, we present two novel algorithms for learning the Minimum Action Distance (MAD) from state trajectories. We also propose a novel quasimetric for learning asymmetric distance estimates, and introduce a set of benchmark domains that model several aspects that make distance learning difficult. In a controlled set of experiments we illustrate that the novel algorithms and proposed quasimetric outperform state-of-the-art algorithms for learning the MAD.

While this work has concentrated on accurately approximating the MAD as a fundamental stepping stone, it opens several promising avenues for future research. First, we will investigate the use of MAD estimates in transfer learning and non-stationary environments, where transition dynamics evolve over time yet maintain a consistent support. On the same line, we are interested in exploring integrating the MAD as a heuristic in search algorithms, particularly in stochastic domains, to identify the properties that make it a robust and informative guidance signal under uncertainty. Having established reliable MAD approximation, we will assess its incorporation into downstream tasks, including goal-conditioned planning and reinforcement learning, to quantify the empirical benefits it brings to complex decision-making problems.

Finally, while MAD can serve as a useful heuristic even in stochastic environments, future work will explore whether it is possible to recover the Shortest Path Distance (SPD) or identify alternative quasimetrics that more closely align with it.

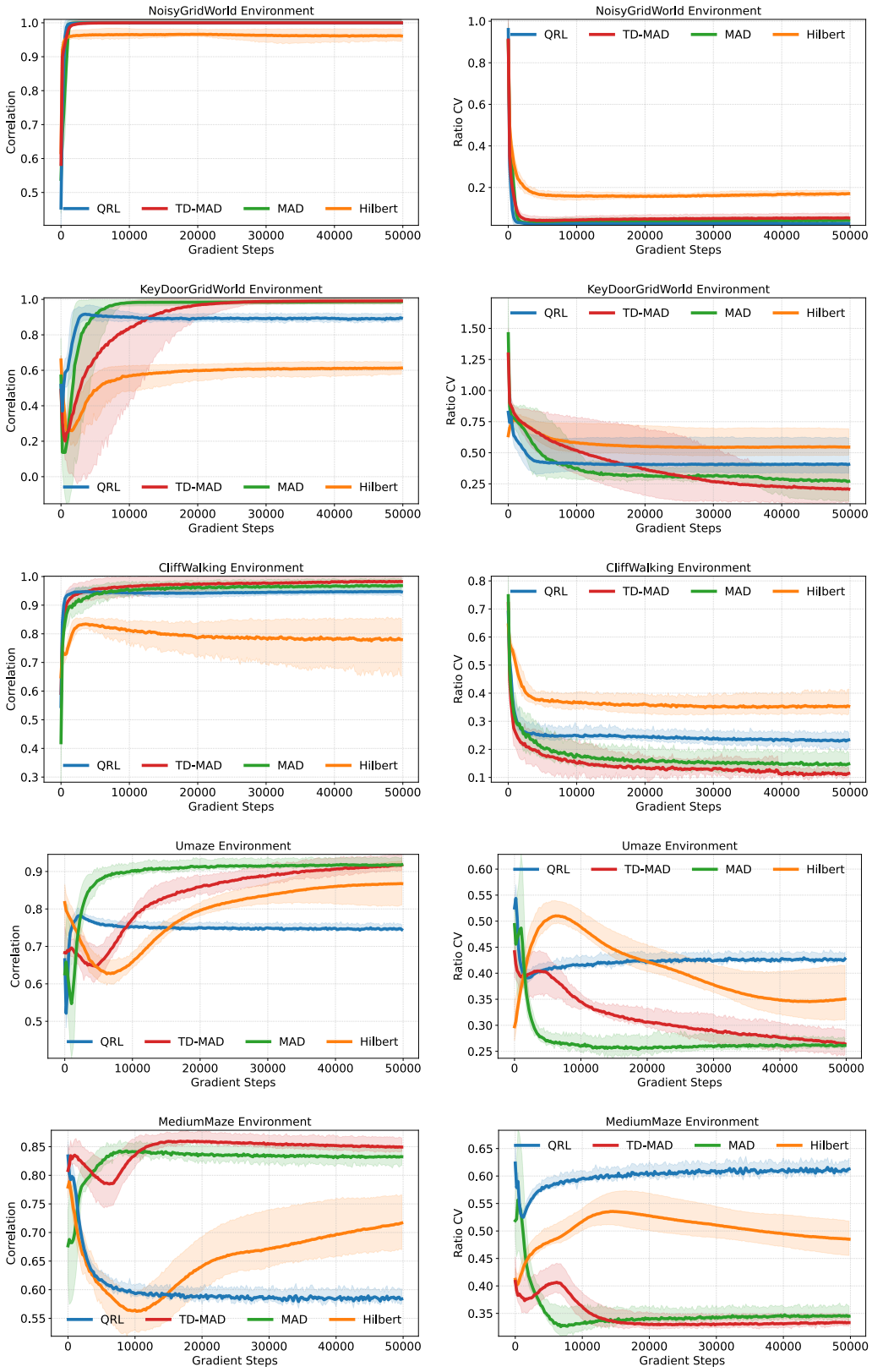

Figure 3: Pearson correlation coefficients and coefficient of variation (CV) ratios across test environments. Shaded regions show the range of values across five random seeds, with upper and lower boundaries representing maximum and minimum values.

References

R. S. Sutton and A. G. Barto. *Reinforcement learning: An introduction*. MIT Press, Cambridge, 1998.

T. Wang, A. Torralba, P. Isola, and A. Zhang. Optimal Goal-Reaching Reinforcement Learning via Quasimetric Learning. In *Proceedings of the 40th International Conference on Machine Learning*, pages 36411–36430. PMLR, 2023.

S. Park, D. Ghosh, B. Eysenbach, and S. Levine. HIQL: Offline Goal-Conditioned RL with Latent States as Actions. In *Advances in Neural Information Processing Systems*, volume 36, pages 34866–34891. Curran Associates, Inc., 2023.

L. Steccanella and A. Jonsson. State Representation Learning for Goal-Conditioned Reinforcement Learning. In *Joint European Conference on Machine Learning and Knowledge Discovery in Databases*, pages 84–99. Springer, 2022.

S. Park, O. Rybkin, and S. Levine. METRA: Scalable Unsupervised RL with Metric-Aware Abstraction. In *Proceedings of the 12th International Conference on Learning Representations*, 2024a.

S. Park, T. Kreiman, and S. Levine. Foundation Policies with Hilbert Representations. In *Proceedings of the 41st International Conference on Machine Learning*, pages 39737–39761. PMLR, 2024b.

D. Ghosh, A. Gupta, A. Reddy, J. Fu, C. M. Devin, B. Eysenbach, and S. Levine. Learning to Reach Goals via Iterated Supervised Learning. In *Proceedings of the 8th International Conference on Learning Representations*, 2020.

J. Tarbouriech, R. Zhou, S. S. Du, M. Pirotta, M. Valko, and A. Lazaric. Stochastic Shortest Path: Minimax, Parameter-Free and Towards Horizon-Free Regret. In *Advances in Neural Information Processing Systems*, volume 34, pages 6843–6855. Curran Associates, Inc., 2021.

L. P. Kaelbling. Learning to Achieve Goals. *International Joint Conference on Artificial Intelligence*, 2:1094–1098, August 1993.

K. Hartikainen, X. Geng, T. Haarnoja, and S. Levine. Dynamical Distance Learning for Semi-Supervised and Unsupervised Skill Discovery. In *Proceedings of the 8th International Conference on Learning Representations*, 2020.

T. Wang and P. Isola. Improved Representation of Asymmetrical Distances with Interval Quasimetric Embeddings. In *NeurIPS Workshop on Symmetry and Geometry in Neural Representations*. Curran Associates, Inc., 2022.

R. Dadashi, S. Rezaeifar, N. Vieillard, L. Hussenot, O. Pietquin, and M. Geist. Offline Reinforcement Learning with Pseudometric Learning. In *Proceedings of the 38th International Conference on Machine Learning*, pages 2307–2318. PMLR, 2021.

P. Dayan. Improving Generalization for Temporal Difference Learning: The Successor Representation. *Neural Computation*, 5(4):613–624, 1993.

A. Barreto, W. Dabney, R. Munos, J. J. Hunt, T. Schaul, H. P. van Hasselt, and D. Silver. Successor Features for Transfer in Reinforcement Learning. In *Advances in Neural Information Processing Systems*, volume 30, pages 4055–4065. Curran Associates, Inc., 2017.

B. Eysenbach, T. Zhang, S. Levine, and R. R. Salakhutdinov. Contrastive learning as goal-conditioned reinforcement learning. *Advances in Neural Information Processing Systems*, 35:35603–35620, 2022.

V. Myers, C. Zheng, A. Dragan, S. Levine, and B. Eysenbach. Learning Temporal Distances: Contrastive Successor Features Can Provide a Metric Structure for Decision-Making. In *Proceedings of the 41st International Conference on Machine Learning*, pages 37076–37096. PMLR, 2024.

S. Yoon, A. Fern, and R. Givan. FF-Replan: A baseline for probabilistic planning. In *Proceedings of the 5th International Conference on Automated Planning and Scheduling (ICAPS)*, pages 352–359, 2007.

R. W. Floyd. Algorithm 97: Shortest Path. *Communications of the ACM*, 5(6):345, June 1962. ISSN 0001-0782.

S. Warshall. A Theorem on Boolean Matrices. *Journal of the ACM*, 9(1):11–12, January 1962. ISSN 0004-5411.

S. Pitis, H. Chan, K. Jamali, and J. Ba. An Inductive Bias for Distances: Neural Nets that Respect the Triangle Inequality. In *Proceedings of the 8th International Conference on Learning Representations*. Curran Associates, Inc., 2020.

J. Fu, A. Kumar, O. Nachum, G. Tucker, and S. Levine. D4RL: Datasets for Deep Data-Driven Reinforcement Learning. *arXiv preprint arXiv:2004.07219*, 2020.

D. P. Kingma and J. Ba. Adam: A method for stochastic optimization. In *Proceedings of the 3rd International Conference on Learning Representations*. PMLR, 2015.

A. L. Maas, A. Y. Hannun, A. Y. Ng, et al. Rectifier nonlinearities improve neural network acoustic models. In *Proc. icml*, volume 30, page 3. Atlanta, GA, 2013.

K. He, X. Zhang, S. Ren, and J. Sun. Deep residual learning for image recognition. In *Proceedings of the IEEE conference on computer vision and pattern recognition*, pages 770–778, 2016.

X. Glorot, A. Bordes, and Y. Bengio. Deep sparse rectifier neural networks. In *Proceedings of the fourteenth international conference on artificial intelligence and statistics*, JMLR Workshop and Conference Proceedings, pages 315–323, 2011.

M. Andrychowicz, F. Wolski, A. Ray, J. Schneider, R. Fong, P. Welinder, B. McGrew, J. Tobin, P. Abbeel, and W. Zaremba. Hindsight Experience Replay. In *Advances in Neural Information Processing Systems*, volume 30. Curran Associates, Inc., 2017.

W. K. Newey and J. L. Powell. Asymmetric Least Squares Estimation and Testing. *Econometrica: Journal of the Econometric Society*, pages 819–847, 1987.

I. Kostrikov, A. Nair, and S. Levine. Offline Reinforcement Learning with Implicit Q-Learning. In *Proceedings of the 10th International Conference on Learning Representations*, 2022.

V. Mnih, K. Kavukcuoglu, D. Silver, A. A. Rusu, J. Veness, M. G. Bellemare, A. Graves, M. Riedmiller, A. K. Fidjeland, G. Ostrovski, et al. Human-level control through deep reinforcement learning. *nature*, 518(7540):529–533, 2015.

H. Van Hasselt, A. Guez, and D. Silver. Deep Reinforcement Learning with Double Q-Learning. In *Proceedings of the AAAI conference on artificial intelligence*, volume 30, 2016.

D. Hendrycks and K. Gimpel. Gaussian Error Linear Units (GELUs). *arXiv preprint arXiv:1606.08415*, 2016.

A Quasimetric Constructions via ReLU Reduction

Let $x, y \in \mathbb{R}^d$. We begin by defining a ReLU-based coordinate reduction, then derive scalar quasimetrics through several aggregation operators, and finally state general results for convex combinations.

A.1 Coordinatewise ReLU Reduction

Definition 1 (ReLU Reduction)**.** *Define the map* $r : \mathbb{R}^d \times \mathbb{R}^d \to \mathbb{R}^d$ *by*

$$r(x, y) = \mathrm{relu}(x - y), \qquad r_i(x, y) = \max\{x_i - y_i, 0\}, \quad i = 1, \ldots, d.$$

Proposition 1. *For all* $x, y, z \in \mathbb{R}^d$ *and* $\lambda > 0$*, each coordinate* r_i *satisfies:*

(a) Nonnegativity and identity: $r_i(x, y) \geq 0$ *and* $r_i(x, x) = 0$.

(b) Asymmetry: $r_i(x, y) \neq r_i(y, x)$ *unless* $x_i = y_i$.

(c) Triangle inequality: $r_i(x, y) \leq r_i(x, z) + r_i(z, y)$.

(d) Positive homogeneity: $r_i(\lambda x, \lambda y) = \lambda\, r_i(x, y)$.

Proof. (a) and (b) follow directly from the definition of the max operation.

(c) Observe that

$$\begin{aligned} r_i(x, y) &= \max(x_i - y_i, 0) = \max\big((x_i - z_i) + (z_i - y_i), 0\big) \\ &\leq \max(x_i - z_i, 0) + \max(z_i - y_i, 0) = r_i(x, z) + r_i(z, y). \end{aligned}$$

(d) Linearity of scalar multiplication inside the max gives

$$r_i(\lambda x, \lambda y) = \max(\lambda x_i - \lambda y_i, 0) = \lambda \max(x_i - y_i, 0) = \lambda r_i(x, y).$$

This concludes the proof. □

A.2 Scalar Quasimetrics via Aggregation

We now obtain real-valued quasimetrics by aggregating the vector $r(x, y)$.

Definition 2 (Max Reduction)**.**

$$d_{\max}(x, y) = \max_{1 \leq i \leq d} r_i(x, y).$$

Definition 3 (Sum and Mean Reductions)**.**

$$d_{\mathrm{sum}}(x, y) = \sum_{i=1}^{d} r_i(x, y), \quad d_{\mathrm{mean}}(x, y) = \tfrac{1}{d} \sum_{i=1}^{d} r_i(x, y).$$

Proposition 2. *Each of* $d_{\max}$*,* d_{sum}*, and* d_{mean} *satisfies for all* $x, y, z \in \mathbb{R}^d$ *and* $\lambda > 0$*:*

(a) Triangle inequality: $d(x, y) \leq d(x, z) + d(z, y)$.

(b) Positive homogeneity: $d(\lambda x, \lambda y) = \lambda\, d(x, y)$.

Proof. (a) follows by combining coordinate-wise triangle bounds with either:

- $d_{\max}$: $\max_i [a_i + b_i] \leq \max_i a_i + \max_i b_i$,
- d_{sum} and d_{mean}: term-wise summation.

(b) is immediate from the linearity of scalar multiplication and properties of max/sum. □

A.3 Convex Combinations of Quasimetrics

More generally, let $d_1, \ldots, d_n$ be any quasimetrics on $\mathbb{R}^d$ each obeying the triangle inequality and positive homogeneity. For weights $\alpha_1, \ldots, \alpha_n \geq 0$ with $\sum_k \alpha_k = 1$, define

$$d_{\text{conv}}(x, y) = \sum_{k=1}^{n} \alpha_k \, d_k(x, y).$$

Proposition 3. *d_{conv} is a quasimetric satisfying:*

(a) Triangle inequality: $d_{\text{conv}}(x, y) \leq d_{\text{conv}}(x, z) + d_{\text{conv}}(z, y)$.

(b) Positive homogeneity: $d_{\text{conv}}(\lambda x, \lambda y) = \lambda \, d_{\text{conv}}(x, y)$.

Proof. Linearity of the weighted sum together with the corresponding property for each d_k yields (a)–(b) immediately. □

B Implementation Details

In this section, we describe the implementation details of each algorithm included in our evaluation.

B.1 Computer Resources

We run all experiments on a single NVIDIA RTX 4070 GPU with 8GB of VRAM and an Intel i7-4700-HX with 32GB of RAM. We will provide the code for all experiments upon acceptance of the paper.

B.2 MAD

To train the MAD distance models, we used the Adam optimizer with a learning rate of 1×10^{-4}, a batch size of 256 for the objective ($\mathcal{L}_o$, $\mathcal{L}_r$), and a separate batch of size 1024 for the constraint loss ($\mathcal{L}_c$). For our main experiment, we used the novel simple quasimetric function and a latent dimension size of 128. We include an ablation over different quasimetric functions and latent dimension sizes in Appendix C.

The full set of hyperparameter values used to train the MAD models can be found in Table 1.

Table 1: Hyperparameters used to train the MAD algorithm.

Hyperparameter	**Value**
Quasimetric Function	d_{simple}
Optimizer	Adam Kingma and Ba (2015)
Learning Rate	1×10^{-4}
Batch Size ($\mathcal{L}_o$, $\mathcal{L}_r$)	128
Batch Size ($\mathcal{L}_c$)	1024
Activation Function (Hidden Layers)	LeakyReLU Maas et al. (2013)
Neural Network	(512, 256, 128) + residual blocks He et al. (2016)
w_r	0.5
w_c	0.1
d_{max}	100
H_c	6

B.3 TDMAD

To train the TDMAD distance models, we used the the Adam optimizer with a learning rate of 1×10^{-4}, a batch size of 256 for the objective ($\mathcal{L}_o$, $\mathcal{L}_r$), and a separate batch of size 1024 for the constraint loss ($\mathcal{L}_c$). For our main experiment, we used the novel simple quasimetric function and a latent dimension size of 128. We include an ablation over different quasimetric functions and latent dimension sizes in Appendix C.

For TDMAD, we remove the hyperparameter $d_{\max}$ from the MAD algorithm, because it is not included in TDMAD's objective ($\mathcal{L}_r$). The temporal-difference update used when training the TDMAD distance models involves the use of a target network, $d_{\theta'}$, which is updated using a Polyak averaging factor $\tau = 0.005$.

The full set of hyperparameter values used to train the TDMAD models can be found in Table 2.

Table 2: Hyperparameters used to train the TDMAD algorithm.

Hyperparameter	**Value**
Quasimetric Function	d_{simple}
Optimizer	Adam Kingma and Ba (2015)
Learning Rate	1×10^{-4}
Batch Size ($\mathcal{L}_o$, $\mathcal{L}_r$)	128
Batch Size ($\mathcal{L}_c$)	1024
Activation Function (Hidden Layers)	LeakyReLU Maas et al. (2013)
Neural Network	(512, 256, 128) + residual blocks He et al. (2016)
w_r	1
w_c	0.1
H_c	6
τ	0.005

B.4 QRL

We trained QRL distance models following the approach of Wang et al. (2023). We used the Lagrangian formulation

$$\min_{\theta} \max_{\lambda \geq 0} -\mathbb{E}_{s,s' \sim S_D}[\phi(d_\theta^{\text{IQE}}(s, s'))] + \lambda \left(\mathbb{E}_{(s,s') \sim p_{\text{transition}}}[\text{relu}(d_\theta^{\text{IQE}}(s, s') + 1)^2] \right), \tag{12}$$

where $\phi(x) \triangleq -\text{softplus}(15 - x, \beta = 0.1)$ is the softplus function with a steepness of 0.1, and $d_\theta^{\text{IQE}}(s, s')$ is the IQE distance between states s and s'. The first term in the objective maximizes the expected distance between states sampled from the dataset, while the second term penalizes distances between state–next-state pairs (s, s') observed in the data.

Through our experiments, we observed that setting the softplus offset to 15 and the steepness to 0.1, as suggested for short-horizon environments by Wang et al. (2023), led to better performance overall.

For the neural network architecture, we used a multi-layer perceptron with an overall layer structure of x - 512 - 512 - 128 (where x is the input observation dimension). Its two hidden layers (each of size 512) use ReLU activations, as described for state-based observations environments (i.e., environments with real vector observations, as opposed to images or other high-dimensional inputs) in the original paper. For the distance function, the resulting 128-dimensional MLP output is fed into a separate 128-512-2048 projector, followed by an IQE-maxmean head with 64 components each of size 32.

The full set of hyperparameter values used to train the QRL distance models can be found in Table 3.

Table 3: Hyperparameters used to train the QRL model.

Hyperparameter	**Value**
Neural Network State embedding	x - 512 - 512 - 128
Neural Network IQE Projector	128-512-2048
Activation Function (Hidden Layers)	ReLU Glorot et al. (2011)
Optimizer	Adam Kingma and Ba (2015)
λ Learning Rate	0.01
Learning Rate Model	1×10^{-4}
Batch Size	256
Quasimetric function	IQE
IQE n components	64
IQE Reduction	maxmean

B.5 Hilbert Representation

A Hilbert representation model is a function $\phi : \mathcal{S} \to \mathbb{R}^d$ that embeds a state $s \in \mathcal{S}$ into a d-dimensional space, such that the Euclidean distance between embedded states approximates the number of actions required to transition between them under the optimal policy.

We trained Hilbert representation models following the approach of Park et al. (2024b), using action-free Implicit Q-Learning (IQL) (Park et al., 2023) and Hindsight Experience Replay (HER) (Andrychowicz et al., 2017).

We used a dataset of state–next-state pairs (s, s'), which we relabeled using HER to produce state–next-state–goal tuples (s, s', g). Goals were sampled from a geometric distribution $\text{Geom}(\gamma)$ over future states in the same trajectory with probability 0.625, and uniformly from the entire dataset with probability 0.375.

We trained the Hilbert representation model ϕ to minimize the temporal-difference loss

$$\mathbb{E}[l_\tau(-\mathbf{1}(s \neq g) - \gamma||\phi(s') - \phi(g)|| + ||\phi(s) - \phi(g)||)]\,, \tag{13}$$

where l_τ denotes the expectile loss (Newey and Powell, 1987), an asymmetric loss function that approximates the $\max$ operator in the Bellman backup (Kostrikov et al., 2022). This objective naturally supports the use of target networks (Mnih et al., 2015) and double estimators (Van Hasselt et al., 2016) to improve learning stability. We included both in our implementation, following the original setup used by Park et al. (2024b).

The full set of hyperparameter values used to train the Hilbert models can be found in Table 4.

Table 4: Hyperparameters used to train the Hilbert representation models.

Hyperparameter	**Value**
Latent Dimension	32
Expectile	0.9
Discount Factor	0.99
Learning Rate	0.0003
Target Network Smoothing Factor	0.005
Multi-Layer Perceptron Dimensions	(512, 512) Fully-Connected Layers
Activation Function (Hidden Layers)	GELU (Hendrycks and Gimpel, 2016)
Layer Normalization (Hidden Layers)	True
Activation Function (Final Layer)	Identity
Layer Normalization (Final Layer)	False
Optimizer	Adam (Kingma and Ba, 2015)
Batch Size	1024

C Ablation Study

In this section, we present additional ablation studies to analyze the performance of our proposed methods. We evaluate the impact of different hyperparameters and design choices on the performance of the learned embeddings.

We conduct experiments in the CliffWalking environment, which is a highly asymmetric environment with a known ground truth MAD. For each experiment we train the MAD algorithm using the same hyperparameters from the main experiments, varying only the hyperparameter of interest whil ekeeping all others fixed. We then evaluate the learned embeddings using Spearman correlation, Pearson correlation, and Ratio CV metrics.

C.1 Effect of Latent Dimension on MAD Accuracy

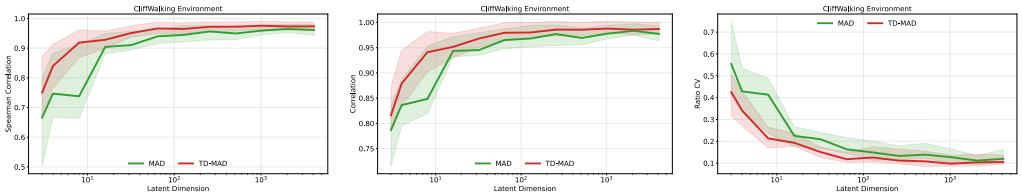

Figure 4: Impact of latent size on Spearman correlation, Pearson correlation and Ratio CV of the MAD and TDMAD algorithms, evaluated in the CliffWalking environment. Shaded regions show the range of values across five random seeds, with upper and lower boundaries representing maximum and minimum values.

Figure 4 shows the impact of the latent dimension size on the performance of our proposed methods. We can see that increasing the latent dimension size improves the performance of our methods. We note that the performance starts to saturate after a latent dimension size of 10, but larger latent dimension sizes still slightly improve the performance and do not harm the performance. This is likely due to the fact that larger latent dimension sizes allow for more expressive representations, which can help to better capture the underlying structure of the environment.

C.2 Effect of Quasimetric Choice on MAD Accuracy

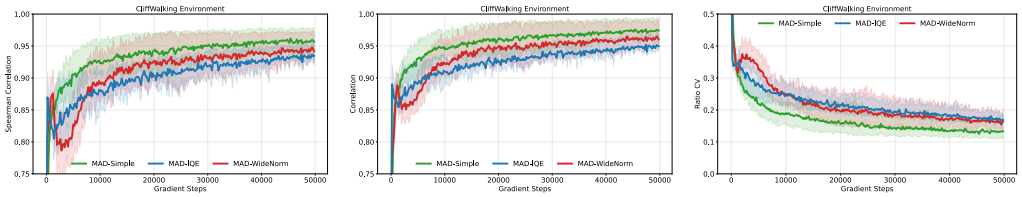

Figure 5: Impact of different quasimetric functions on correlation and Ratio CV of the MAD algorithm, evaluated in the CliffWalking environment. Shaded regions show the range of values across five random seeds, with upper and lower boundaries representing maximum and minimum values.

Figure 5 shows the impact of different quasimetric functions on the performance of the learned MAD model. The novel simple quasimetric (MAD-Simple) achieves the best performance, outperforming both the Wide Norm (MAD-WideNorm) and IQE (MAD-IQE) variants. While Wide Norm and IQE perform similarly to each other, they consistently underperform the simple quasimetric across all three evaluation metrics.

Figure 6 presents the same ablation over quasimetric functions, now applied to learning the TDMAD model. The results mirror the previous setting: the simple quasimetric (TD-MAD-Simple) again achieves the strongest performance, while the Wide Norm (TD-MAD-WideNorm) and IQE (TD-MAD-IQE) variants lag slightly behind and show comparable results to each other.

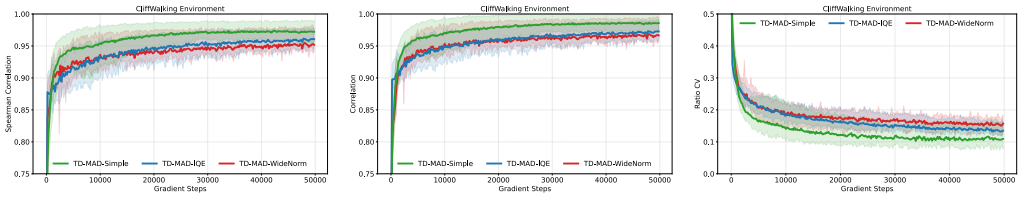

Figure 6: Impact of different quasimetric functions on correlation and Ratio CV of the TDMAD algorithm, evaluated in the CliffWalking environment. Shaded regions show the range of values across five random seeds, with upper and lower boundaries representing maximum and minimum values.

In this experiment, we used a latent dimension size of 256. For the Wide Norm quasimetric, we configure the model with 32 components, each having an output component size of 32. For the IQE quasimetric, we set each component to have a dimensionality of 16. For both quasimetric functions we use maxmean reduction (Pitis et al., 2020).

C.3 Effect of Dataset Size on MAD Accuracy

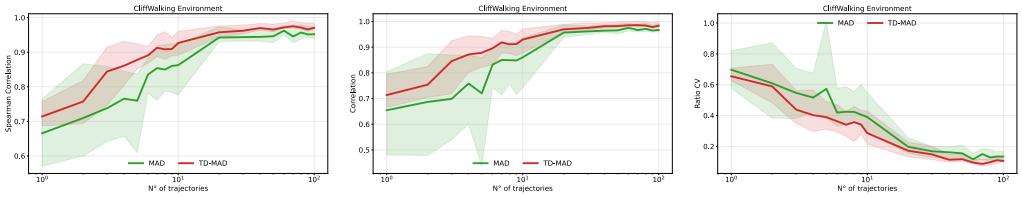

Figure 7: Impact of dataset size on Spearman correlation, Pearson correlation and Ratio CV of the MAD and TDMAD algorithms, evaluated in the CliffWalking environment. Shaded regions show the range of values across five random seeds, with upper and lower boundaries representing maximum and minimum values.

Figure 7 illustrates how dataset size affects the performance of our proposed methods. As the number of trajectories increases, the dataset provides broader coverage of all the possible transitions in the environment, leading to a more accurate approximation of the MAD.

C.4 Complete list of results

In this section we report the complete list of results including the Spearman Correlation metric, and contrast them with the Pearson Correlation for reference. The results appear in Figure 8.

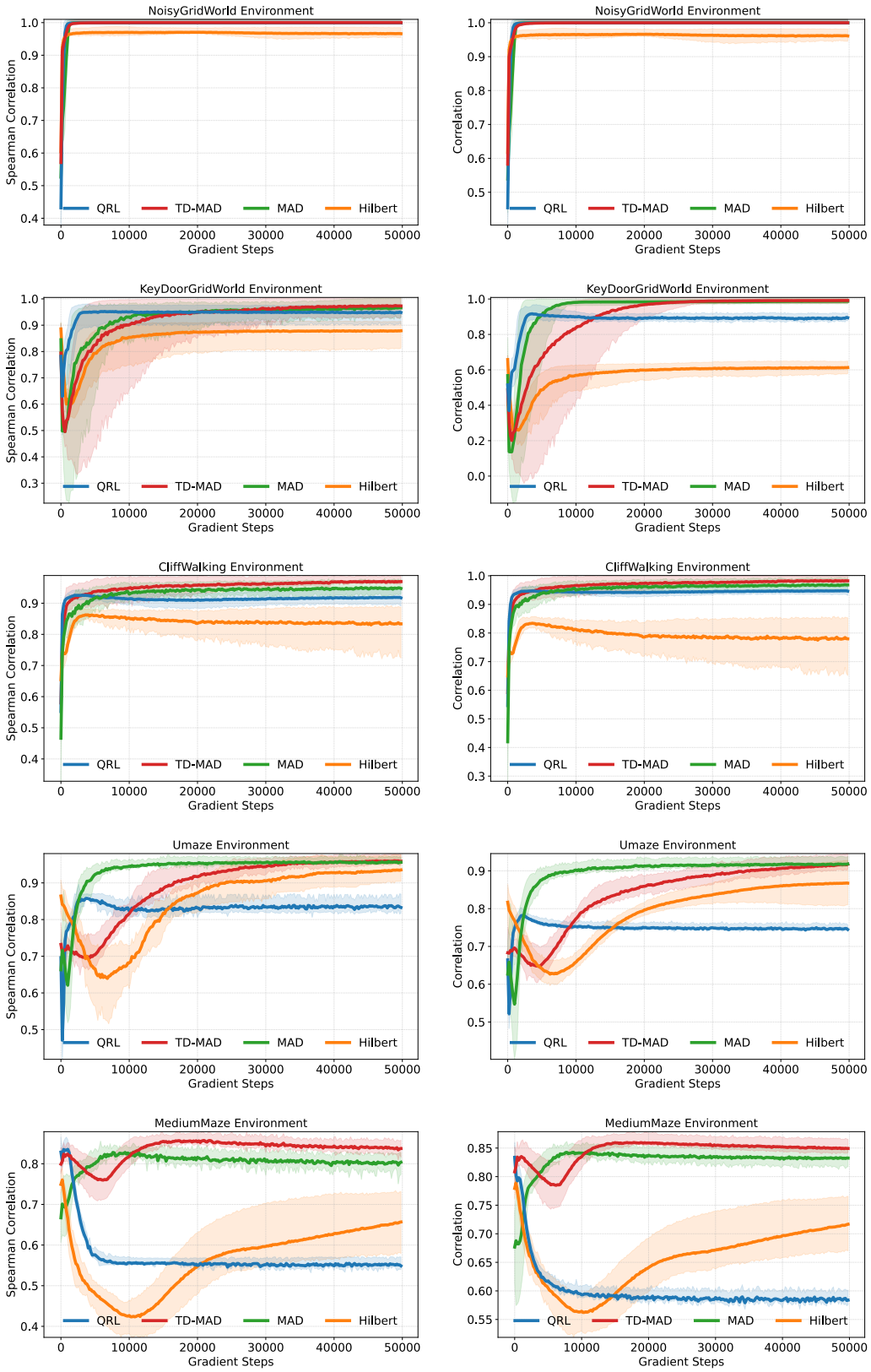

Figure 8: Spearman correlation and Pearson correlation coefficients across test environments. Shaded regions show the range of values across five random seeds, with upper and lower boundaries representing maximum and minimum values.

D Environments

Our test environments were specifically chosen to span a comprehensive range of reward-free MDP characteristics and challenges, ensuring a thorough evaluation. Key design considerations for this suite include:

- *Noisy Observations:* To assess robustness to imperfect state information, which can challenge algorithms relying on precise state identification.
- *Stochastic Dynamics:* To evaluate if our algorithm can retrieve the MAD even when transitions are not deterministic. This reflects real-world scenarios where environments have inherent randomness or agent actions have uncertain outcomes.
- *Asymmetric:* To test the capability of our algorithm to learn true quasimetric distances that capture directional dependencies (e.g., one-way paths, key-door mechanisms).
- State Spaces:
  - *Continuous State Spaces:* To demonstrate applicability to problems with real-valued state representations where function approximation is essential.
  - *Discrete State Spaces:* To provide foundational testbeds with clearly defined structures and allow for exact MAD computation.
- Action Spaces:
  - *Continuous Action Spaces:* To evaluate performance in environments where actions are defined by real-valued parameters, common in robotics and physical control tasks.
  - *Discrete Action Spaces:* To ensure applicability to environments with a finite set of distinct actions.
- *Complex Dynamics:* Incorporating environments like PointMaze, which feature non-trivial physics (velocity, acceleration).
- *Hard Exploration:* Utilizing environments with complex structures (e.g., intricate mazes) that pose significant exploration challenges for naive data collection policies (like the random policy we used in our experiments).

NoisyGridWorld

Noisy Observations, Stochastic Dynamics, Continuous State Space, Discrete Action Space

- **State space:** The agent receives a 4-dimensional observation vector (x, y, n_1, n_2)at each step. In this observation, (x, y) are discrete coordinates in a 13×13 grid, and $(n_1, n_2) \sim \mathcal{N}(0, \sigma^2 I)$ are i.i.d. Gaussian noise components. The true underlying latent state, which is not directly observed by the agent in its entirety without noise, is the coordinate pair (x, y). The presence of the noise components (n_1, n_2) in the observation makes the sequence of observations non-Markovian with respect to this true latent state.
- **Action space:** Four stochastic actions are available in all states: `UP`, `DOWN`, `LEFT`, and `RIGHT`.
- **Transition dynamics:** With probability 0.5, the intended action is executed; with probability 0.5, a random action is applied. Transitions are clipped at grid boundaries.
- **Initial state distribution (μ_0):** The agent's initial true latent state (x_0, y_0) is a random real-valued position sampled uniformly from the grid. The full initial observation is $(x_0, y_0, n_{1,0}, n_{2,0})$, where the initial noise components $(n_{1,0}, n_{2,0})$ are also sampled i.i.d. from $\mathcal{N}(0, \sigma^2 I)$. The real-valued nature of both the initial position and the noise components makes the observed state space continuous.
- **Ground-truth MAD:** Since the latent state is deterministic apart from noise, the MAD between two states (x_1, y_1) and (x_2, y_2) is the Manhattan distance $|x_1 - x_2| + |y_1 - y_2|$. Noise components are ignored.

KeyDoorGridWorld

Asymmetric, Deterministic Dynamics, Discrete State Space, Discrete Action Space

- **State space:** States are triples (x, y, k), where (x, y) is the agent's position in a 13×13 grid, and $k \in \{0, 1\}$ indicates whether the key has been collected.
- **Action space:** Four deterministic actions are available in all states: `UP`, `DOWN`, `LEFT`, and `RIGHT`.
- **Transition dynamics:** Transitions are deterministic. The agent picks up the key by visiting the key's cell; the key cannot be dropped once collected. The door can only be passed if the key has been collected.
- **Initial state distribution (μ_0):** The agent starts at position $(1, 1)$.
- **Ground-truth MAD:** Defined as the minimum number of steps to reach the target state, accounting for key dependencies. For example, if the agent lacks the key and the goal requires it, the path must include visiting the key first.

CliffWalking

Asymmetric, Deterministic Dynamics, Discrete State Space, Discrete Action Space

- **State space:** The environment is a 4×12 grid. Each state corresponds to a discrete cell (x, y).
- **Action space:** Four deterministic actions are available in all states: `UP`, `DOWN`, `LEFT`, or `RIGHT`.
- **Transition dynamics:** Transitions are deterministic unless the agent steps into a cliff cell, in which case it is returned to the start. The episode is not reset.
- **Initial state distribution (μ_0):** The agent starts at position $(1, 1)$.
- **Ground-truth MAD:** The MAD is the minimal number of steps required to reach the target state, allowing for cliff transitions. Since falling into the cliff resets the agent's position, it can create shortcuts and lead to strong asymmetries in the distance metric.

PointMaze

Continuous State Space, Complex Dynamics, Hard exploration, Continuous Action Space

- **State space:** The agent observes a 4-dimensional vector $(x, y, \dot{x}, \dot{y})$, where (x, y) is the position of a green ball in a 2D maze and $(\dot{x}, \dot{y})$ are its linear velocities in the x and y directions, respectively.
- **Action space:** Continuous control inputs (a_x, a_y) corresponding to applied forces in the x and y directions. The applied force is limited to the range $[-1, 1]$ N in each direction.
- **Transition dynamics:** The system follows simple force-based dynamics within the MuJoCo physics engine. The applied forces affect the agent's velocity, which in turn updates its position. The ball's velocity is limited to the range $[-5, 5]$ m/s in each direction. Collisions with the maze's walls are inelastic: any attempted movement through a wall is blocked.
- **Initial state distribution (μ_0):** The agent starts at a random real-valued position (x, y) sampled uniformly from valid maze locations. The initial velocities $(\dot{x}_0, \dot{y}_0)$ are set to $(0, 0)$.
- **Ground-truth MAD:** The maze is discretized into a uniform grid. Using the Floyd-Warshall algorithm on the resulting connectivity graph, we compute shortest path distances between all reachable pairs of positions.